

Homogeneous and inhomogeneous contributions to the luminescence linewidth of point defects in amorphous solids: Quantitative assessment based on time-resolved emission spectroscopy

Michele D'Amico,^{1,2,*} Fabrizio Messina,¹ Marco Cannas,¹ Maurizio Leone,^{1,2} and Roberto Boscaino¹

¹*Dipartimento di Scienze Fisiche ed Astronomiche, Università di Palermo, Via Archirafi 36, I-90123 Palermo, Italy*

²*Istituto di Biofisica, U. O. di Palermo, Consiglio Nazionale delle Ricerche, Via Ugo La Malfa 153, I-90146 Palermo, Italy*

(Received 21 March 2008; revised manuscript received 4 June 2008; published 3 July 2008)

This paper describes an experimental method that allows the estimation of the inhomogeneous and homogeneous linewidths of the photoluminescence band of a point defect in an amorphous solid. We performed low-temperature time-resolved luminescence measurements on two defects chosen as model systems for our analysis: extrinsic oxygen deficient centers [ODC(II)] in amorphous silica and F_3^+ centers in crystalline lithium fluoride. Measurements evidence that only defects embedded in the amorphous matrix feature a dependence of the radiative decay lifetime on the emission energy and a time dependence of the first moment of the emission band. A theoretical model is developed to link these properties to the structural disorder typical of amorphous solids. Specifically, the observations on ODC(II) are interpreted by introducing a Gaussian statistical distribution of the zero-phonon line energy position. Comparison with the results obtained on F_3^+ crystalline defects strongly confirms the validity of the model. By analyzing experimental data within this frame, we obtain separate estimations of the homogeneous and inhomogeneous contributions to the measured total linewidth of ODC(II), which turns out to be mostly inhomogeneous.

DOI: [10.1103/PhysRevB.78.014203](https://doi.org/10.1103/PhysRevB.78.014203)

PACS number(s): 71.55.Jv, 61.72.jn, 78.55.Qr, 78.47.Cd

I. INTRODUCTION

The physics of color centers embedded in a solid matrix is a fundamental and interesting scientific field both from the point of view of basic physics and for their wide technological applications as modifiers of the macroscopic physical properties of solids (e.g., optical transparency, refractive index, and electrical resistance).^{1,2} A large body of experimental evidence has led to general agreement on the fact that the properties of point defects may be significantly different depending on the crystalline or amorphous structure of the solid they are embedded in.³ Indeed, in a crystal each member of an ensemble of identical defects experiences the same local environment. As a consequence, every spectroscopical property of the ensemble of defects, such as the line shape of the related absorption or photoluminescence (PL) bands, can be interpreted as a property of the single center and is referred to as *homogeneous*. The homogeneous absorption linewidth is mainly determined by the electron-phonon interaction and it is related to other important physical properties of the defect, such as the Huang-Rhys factor and the phonon vibrational frequencies.^{2,3} On the other hand, defects in an amorphous solid are believed to feature site-to-site statistical distributions of the spectroscopic properties due to the disorder of the surrounding matrix. Hence, the line shapes of their optical bands are characterized by an *inhomogeneous* broadening,²⁻⁴ which reflects the degree of disorder of the amorphous solid and concurs, together with the homogeneous effects, to determine the overall spectroscopic signature of the color center.

Many experimental approaches have been proposed to estimate the homogeneous and inhomogeneous contributions to the experimental linewidth of an optically active center: exciton resonant luminescence, resonant second-harmonic scattering, femtosecond photon echo, spectral hole burning, and site-selective spectroscopy.⁴⁻⁹ However, the issue is still

open since none of these techniques is applicable to the whole variety of inhomogeneous physical systems of interest. For instance, in amorphous solids, site-selective spectroscopy can be successfully applied only to defects which allow the direct observation of the zero-phonon line (ZPL) by virtue of a weak coupling with the vibrational modes of the matrix.^{3,8}

In this paper we propose an alternative experimental approach to this problem, which allows the estimation of the inhomogeneous and homogeneous linewidths based on mapping the variations of the radiative decay lifetime within an inhomogeneously broadened luminescence emission band by time-resolved laser-excited luminescence. For this purpose, in Sec. II we first describe an adapted version of the theoretical treatment of the optical properties of a point defect in a solid, which takes into account the effects of heterogeneity in amorphous systems. Next, in Sec. IV we demonstrate that the predictions of our model are consistent with the results of measurements performed on two model point defects, one in a crystal solid and the other one in a glass. Finally, we use the theoretical model to estimate the inhomogeneous and homogeneous widths of the two model defects and to obtain other physical parameters of interest.

II. THEORETICAL DESCRIPTION OF OPTICAL DEFECT PROPERTIES

We briefly review the standard theoretical description of the optical properties of a point defect in a crystal¹⁻³ in order to adapt it later to the case of amorphous systems. In addition to the crude *Born-Oppenheimer* and *Franck-Condon* approximations, we suppose the defect to be coupled with only one vibrational mode of the solid matrix of frequency ω_p , assumed to be the same for ground and excited electronic states. The frequency ω_p can be regarded also as the mean frequency of the vibrational modes of the solid or can be

thought as the “effective” phonon frequency coupled with the electronic transition.¹⁰

In this frame, the absorption cross section $\Omega(E)$ of a defect as a function of the excitation energy E at the absolute zero temperature is given by^{3,10}

$$\Omega(E) = \beta \sum_k |M_{0k}|^2 E \delta[E - (E_0 + k\hbar\omega_p)], \quad (1)$$

where δ indicates a Dirac delta function. The summation is carried out over the vibronic transitions linking the ground electronic state with zero phonons toward different vibrational sublevels (k) of the electronic excited state, spaced by $\hbar\omega_p$. The energy value E_0 (zero-phonon line) is the absorption transition without emission or absorption of phonons. M_{0k} is the overlap integral between nuclear wave functions associated with the ground and excited states, while β is given by $\beta = \frac{1}{n} \left(\frac{E_{\text{eff}}}{E_{\text{ext}}} \right)^2 \frac{4\pi^2}{3\hbar c g_l} |D|^2$, where D is the matrix element of the electric dipole operator between the ground and excited electronic states and g_l is the degeneracy of the lower electronic state. The effective field correction $\frac{1}{n} \left(\frac{E_{\text{eff}}}{E_{\text{ext}}} \right)^2$ accounts for the polarization effect induced by the external field on the solid.¹³ We assume here that the refraction index n is constant in the electromagnetic range investigated. In the harmonic approximation for the vibrational sublevels relative to the ground and excited states, the $|M_{0k}|^2$ coefficients are given by a Poisson distribution:³

$$|M_{0k}|^2 = e^{-H} \frac{H^k}{k!}, \quad (2)$$

where H is the *Huang-Rhys factor*, expressing the number of phonons emitted by the system after absorption of a photon while relaxing to the ground vibrational substate of the excited electronic level.¹ Given a population of identical defects, the envelope of the δ functions in Eq. (1) describes their characteristic *homogeneous* absorption line shape, with (aside from the effect of the factor E) $E_{\text{Abs}} = E_0 + H\hbar\omega_p$ as the first moment and $\sigma_{\text{ho}} = \sqrt{H\hbar\omega_p}$ as the half width, related to the full width at half maximum (FWHM) as $\text{FWHM} \approx 2.35\sigma_{\text{ho}}$.

After relaxation toward the bottom of excited electronic state, the system can relax back to the ground state by spontaneous photon emission (photoluminescence). The following relationship of *mirror symmetry* links the absorption $\Omega(E)$ and luminescence $L(E)$ band shapes:³

$$\frac{L(E)}{E^3} \propto \frac{\Omega(2E_0 - E)}{2E_0 - E}. \quad (3)$$

The energy difference between absorption and emission peaks (*Stokes shift*) is linked to the Huang-Rhys factor and results to $2S = 2H\hbar\omega_p$. Using mirror-symmetry equation (3) and Eq. (1), we obtain

$$L(E) \propto \beta \sum_k |M_{0k}|^2 E^3 \delta[E - (E_0 - k\hbar\omega_p)], \quad (4)$$

which represents the *homogeneous* emission line shape, with (aside from the effect of the factor E^3) $E_{\text{em}} = E_0 - H\hbar\omega_p$ as the first moment and σ_{ho} as the half width. Expression (4) does

not take into account the dependence from the excitation energy within the absorption band. This is based on experimental results and it will be discussed later.

The PL radiative lifetime τ is linked to the absorption profile by *Forster's equation*:^{3,11}

$$1/\tau = \frac{n^2}{\pi^2 c^2 \hbar^3} \frac{g_l}{g_u} \int (2E_0 - E)^3 \frac{\Omega(E)}{E} dE, \quad (5)$$

where g_u is the degeneracy of the upper electronic state. Combining Eqs. (5) and (1), we obtain the decay rate $1/\tau$:

$$1/\tau = \gamma \sum_k |M_{0k}|^2 (E_0 - k\hbar\omega_p)^3, \quad (6)$$

where $\gamma = \frac{n^2}{\pi^2 c^2 \hbar^3} \frac{g_l}{g_u} \beta$. The cubic dependence appearing in the above expression is a direct consequence of the relation between Einstein coefficients for absorption and spontaneous emission, which forms the basis of Forster's equation. Equation (6) can be often approximated by neglecting the contributions far from $k \sim H$, thus obtaining

$$1/\tau \sim \gamma (E_0 - S)^3. \quad (7)$$

This expression shows that the decay rate is proportional to γ and approximately to the third power of the first moment of the emission band.

Summing up, the global expression for the luminescence of a population of identical point defects in a solid matrix as a function of the spectral position E and time t after an exciting light pulse (*homogeneous shape*) is

$$L(E, t) \propto \gamma \sum_k |M_{0k}|^2 E^3 e^{-t/\tau} \delta[E - (E_0 - k\hbar\omega_p)]. \quad (8)$$

This expression assumes that nonradiative channels from the excited state are absent. As we see from Eq. (8), the shape and kinetics of the homogeneous luminescence band are completely characterized by four parameters: E_0 (the ZPL position), $\hbar\omega_p$ (the phonon energy), γ (proportional to $|D|^2$), and H (the Huang-Rhys factor). H and $\hbar\omega_p$ can be expressed in terms of the half Stokes shift S and of the homogeneous half width σ_{ho} : $\hbar\omega_p = \sigma_{\text{ho}}^2/S$ and $H = S^2/\sigma_{\text{ho}}^2$. In this way, expression (8) can be alternatively regarded as depending on the four parameters E_0 , S , σ_{ho} , and γ ; thus it is indicated by the expression $L(E, t|E_0, S, \sigma_{\text{ho}}, \gamma)$.

For defects in an amorphous matrix, we can argue the hypothesis of a population of identical defects to fail. Indeed, each point defect interacts with different environments and it is possible that this conformational heterogeneity causes a site-to-site statistical distribution of one or more of the homogeneous properties of single defects. The simplest model we can put forward to take into account the disorder effects is to introduce a Gaussian distribution of the ZPL position E_0 , peaked at \widehat{E}_0 and with an inhomogeneous half width σ_{in} ; in this scheme, γ , S , and σ_{ho} are still considered as undistributed parameters. Within these hypotheses, the global PL signal $L^*(E, t)$ emitted by the ensemble of nonidentical point defects can be now expressed as the convolution of the homogeneous shape $L(E, t)$ with the inhomogeneous distribution of E_0 :

$$L^*(E, t | \widehat{E}_0, \sigma_{\text{in}}, S, \sigma_{\text{ho}}, \gamma) \propto \int L(E, t | E_0, S, \sigma_{\text{ho}}, \gamma) \times e^{[-(E_0 - \widehat{E}_0)^2 / 2\sigma_{\text{in}}^2]} dE_0. \quad (9)$$

Equations (8) and (9) lead us to predict a difference between the PL signals of defects in crystalline and amorphous solids. Indeed, when the inhomogeneous broadening σ_{in} is almost zero, as expected for point defects in a crystalline matrix, Eq. (8) has to be used, and the radiative lifetime τ should be independent from the spectral position at which it is measured within the emission band. In fact, τ is expressed by Eq. (6), which is a function of the homogeneous parameters E_0 , γ , S , and σ_{ho} , expected to be the same for all defects in the solid. In contrast, in an amorphous solid a PL band due to an ensemble of point defects can be thought of as arising from the overlap of several bands with different E_0 as described by Eq. (9) and thus featuring different lifetimes. Hence, when σ_{in} is comparable with σ_{ho} , it should be possible to experimentally observe a dispersion in τ by measuring the decay of the PL signal at different emission energies. Also, the shape of a band arising from the overlap of subbands with different lifetimes should vary in time, so that the position of its first moment $M_1(t)$, calculated by the usual expression

$$M_1(t) = \frac{\int EL^*(E, t) dE}{\int L^*(E, t) dE}, \quad (10)$$

should depend on time. Therefore, both the dispersion of τ within the emission band and the time dependence of the first moment can be used in principle as experimental probes of inhomogeneous effects.

It is worth noting that according to Eq. (7), τ strongly depends on the first moment of the emission band, $E_{\text{em}} = E_0 - S$, and more weakly on γ . This leads to E_0 as the parameter of choice to be distributed in our model. Moreover, a Gaussian distribution of E_0 was experimentally demonstrated for the nonbridging oxygen hole center point defect in silica, for which the zero-phonon line can be directly observed by site-selective spectroscopy at low temperatures.^{8,12} On the other hand, we acknowledge that similar predictions can be obtained by introducing a distribution of the half Stokes shift S with an undistributed E_0 . Data reported later on in this paper do not allow discrimination between these two possibilities.

Finally, to get further insight into the meaning of Eq. (9), it is useful to consider the case in which the inhomogeneous half width is much larger than the homogeneous one. In this case, the inhomogeneous line shape is a slowly varying function as compared to the homogeneous term $L(E, t)$ so that, to the purposes of integration, the latter can be approximated as $\delta[E - (E_0 - S)]e^{-t/\tau}$, with τ given by Eq. (7). By substituting in Eq. (9), we get

$$L^*(E, t) \propto e^{-\gamma E^3 t} e^{-[(E + S - \widehat{E}_0)]^2 / 2\sigma_{\text{in}}^2}. \quad (11)$$

This expression predicts an exponential decay whose τ depends cubically from the experimental observation energy E within the inhomogeneous band.

In the intermediate situation of non-negligible homogeneous half width, Eq. (9) deviates in principle from a single exponential decay, as it contains contributions with different values of τ . However, we verified that the typical values of the parameters, which will be used in the following to fit experimental data (\widehat{E}_0 , σ_{in} , S , σ_{ho} , and γ), correspond to predicted decay curves that always remain very close to single exponential for all practical purposes. From a theoretical point of view, we can define in general $\tau(E)$ as the time in which $L^*(E, t)$ (at a fixed E) decreases by a $1/e$ factor from $L^*(E, 0)$. With this definition, we can summarize the above considerations as follows: The $\tau(E)$ curve (with E varying within the observed emission band) is expected to vary progressively from a constant value (for a completely homogeneous system) to a cubic dependence (for a completely inhomogeneous system) with increasing ratio of inhomogeneous to homogeneous width. To check the validity of our model, we have performed experimental measurements (described in the following) on crystalline and amorphous defects.

III. MATERIALS AND EXPERIMENTAL METHODS

We chose F -type centers in lithium fluoride (LiF) and oxygen deficient centers of the second type, ODC(II), in amorphous silicon dioxide (SiO₂, or silica) as model point defects on which testing our approach. Both centers feature broad near-Gaussian luminescence bands in the ultraviolet (UV) range with close decay lifetime values (~ 8 ns), and they have both been widely studied in literature because of their important technological applications. Specifically, LiF is a material traditionally employed in the production of high-quality optical elements to be used in the infrared, visible, and particularly in the ultraviolet spectral regions. F -type centers in LiF (electron trapped in anion vacancies) are the subject of active investigation in the areas of color center lasers, radiation dosimetry, and integrated optics (see Ref. 13 and references therein). The study of point defects in silica is a fundamental technological problem as well because their presence compromises the optical and electrical properties of glasses in their wide uses as optical components and as insulators in metal-oxide-semiconductor transistors and for guiding or processing light signals (optical fibers and Bragg gratings).^{2,3} ODC(II) is a peculiar defect of the amorphous phase of SiO₂.^{3,14} Thus it is an interesting model system in which to investigate the characteristic properties of defects in disordered materials with respect to crystalline ones. Its microscopic structure consists of an atom bonded to two oxygen atoms of the matrix ($=X^{**}$), where X is an atom belonging to the isoelectronic series of Si, Ge, and Sn.^{3,14,15} Previous studies have suggested that the spectroscopic properties of ODC(II) are significantly conditioned by inhomogeneous effects.¹⁶⁻¹⁹

We report measurements performed on two samples: the first one is a crystalline lithium fluoride sample, hereafter denoted as LiF. Prior to any measurement this specimen, $5 \times 5 \times 1.25$ mm³ sized, was irradiated at room temperature with electrons of 3 MeV energy for a total dose of 1.5×10^6 rad. The purpose of irradiation was to induce in the sample the formation of luminescent F -type centers. The sec-

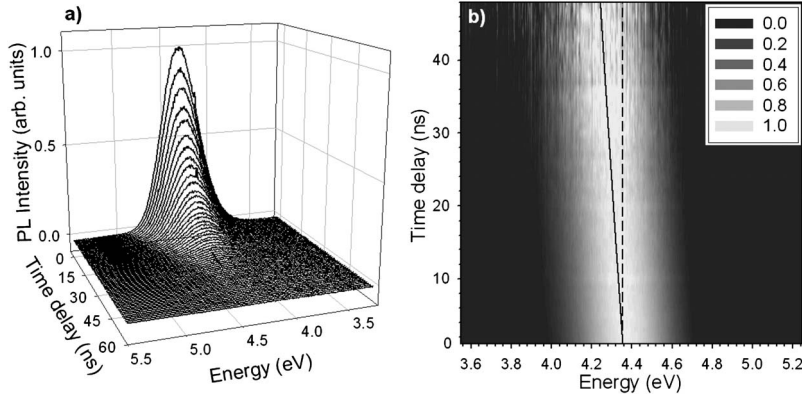


FIG. 1. (a) Decay of the luminescence band of Ge-ODC(II) centers in the I301 sample, excited at 240 nm at $T=25$ K. (b) Normalized data of panel (a) in a contour plot. The continuous line corresponds to the position of the first moment of the PL band as a function of time. The position of the first moment at $t_D=0$ is reported (dashed line) as a reference.

ond sample is a fused silica (commercial name: Infrasil301, provided by Heraeus Quartzglas;²⁰ $5 \times 5 \times 1$ mm³ sized), hereafter named I301, manufactured by fusion and quenching of natural quartz, with typical concentration of impurities of ~ 20 ppm in weight.²⁰ In particular, as-grown I301 contains an ~ 1 ppm concentration of Ge impurities, due to contamination of the quartz from which the material was produced. Previous studies demonstrated that in the as-grown material, most of the Ge impurities are arranged as Ge-ODC(II) defects (=Ge^{**}); moreover, the close resemblance between the optical properties of I301 and sol-gel silica samples doped with Ge atoms ensures us that in I301 sample the contribution to PL of intrinsic Si-ODC(II) defects is negligible.^{14,21} The optical activity of Ge-ODC(II) at low temperature (<100 K) consists of an absorption band centered at ~ 5.1 eV, which excites a fast (lifetime in the nano-second range) emission band centered at ~ 4.3 eV, due to the inverse transition.^{10,14,22}

PL measurements were done in a standard backscattering geometry, under excitation by a pulsed laser (Vibrant Opotek; pulse width of 5 ns, repetition rate of 10 Hz, energy density per pulse of 0.30 ± 0.02 mJ/cm²) tunable in the UV-visible range. The luminescence emitted by the sample was dispersed by a spectrograph (SpectraPro 2300i, PI/Acton, 300 mm focal length) equipped with three different gratings, and detected by an air-cooled intensified charge-coupled device (CCD; PIMAX, PI/Acton). The detection system can be triggered in order to acquire the emitted light only in a given temporal window defined by its width (t_W) and by its delay t_D from the end of the laser pulse. All measurements reported here were performed on samples kept at 25 K in high vacuum ($\sim 10^{-6}$ mbar) within a He flow cryostat (Optistat CF-V, Oxford Instruments). All luminescence signals in I301 were acquired with a 300 grooves/mm grating with a 2 nm bandwidth, while the signals in LiF were measured with a 150 grooves/mm grating with a 2.5 nm bandwidth. All the spectra were corrected for the spectral response and for the dispersion of the detection system.

IV. EXPERIMENTAL RESULTS

In Fig. 1(a) we show a typical time-resolved measurement of the PL activity of Ge-ODC(II) in the I301 sample, performed at 25 K under laser excitation at 240 nm (5.17 eV). The PL decay was analyzed by performing 60 acquisitions

with the same integration time $t_W=1$ ns but at different delays t_D , going from 0 to 60 ns from the laser pulse. Figure 1(b) shows the normalized spectra of panel (a) in a contour plot and evidences that the first moment of the band (continuous line) varies in time.

In Fig. 2(a) we report the signal acquired for $t_D=0$, corresponding to the first spectrum in Fig. 1(a). The PL band of Ge-ODC(II), as acquired immediately after the end of the laser pulse, is peaked at ~ 4.4 eV and has an ~ 0.45 eV FWHM, consistent with literature data.¹⁴ Completely analogous time-resolved measurements were carried out on the PL activity of F -type centers in the LiF sample.

This specimen was excited at 450 nm (2.76 eV) and its luminescence was collected by varying t_D from 0 to 100 ns with $t_W=1$ ns. We report in Fig. 2(b) the luminescence signal detected in LiF at $t_D=0$. It is apparent that the PL signal of LiF comprises two contributions peaked at ~ 2.3 and ~ 1.8 eV. These signals are known to be associated with two different defects, the F_3^+ and F_2^- centers respectively, both consisting of aggregates of F -type centers.^{13,23} In particular, the main ~ 2.3 eV band with a ~ 0.27 eV FWHM is due to

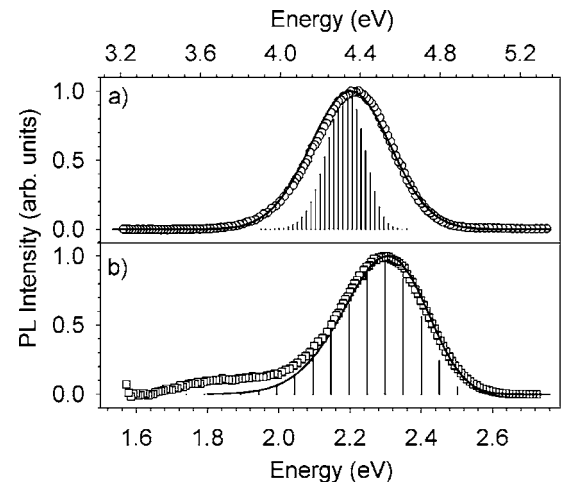


FIG. 2. Low-temperature (25 K) luminescence of Ge-ODC(II) in the I301 sample (a) and of F centers in the LiF sample (b). Both PL bands are obtained by exciting at the maximum of the respective absorption bands and acquired for $t_D=0$ and with $t_W=1$ ns. The continuous line is the result of the fitting procedure by our theoretical model. The Poissonian homogeneous shape is also shown (see discussion).

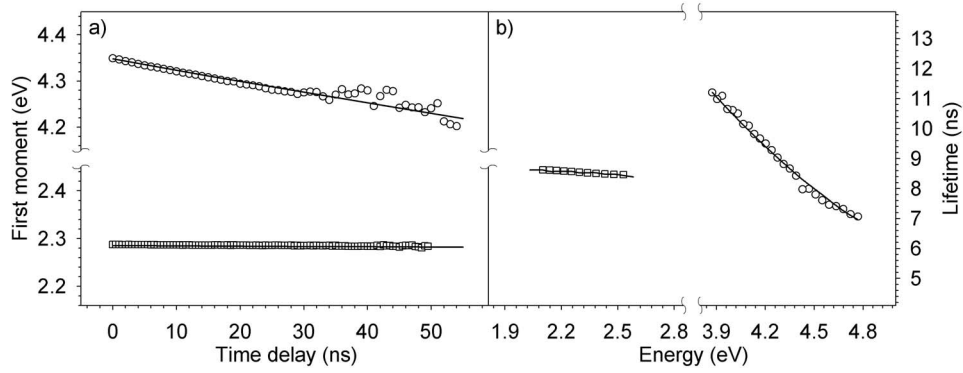


FIG. 3. (a) First moment of the emission band of Ge-ODC(II) (white circles) and of F_3^+ (white squares). (b) Decay lifetime as estimated by fitting with exponential function data at different emission energies within the emission band of the Ge-ODC(II) centers in the I301 sample (white circles) and of the F_3^+ in the LiF sample (white squares). The continuous lines are the results of the fitting procedure by our theoretical model (see discussion).

F_3^+ , consisting of two electrons localized on three adjacent anion vacancies.¹³ For each activity [Ge-ODC(II) and F_3^+], one can extract the time dependence of the first moment of the luminescent bands from the time-resolved measurements [e.g., those in Fig. 1 in the case of Ge-ODC(II)]. Data thus obtained are reported in Fig. 3(a). The origin of the time scale corresponds to $t_D=0$.

We observe that the PL activity in silica shows an approximately linear decrease in the first moment as a function of time. In contrast, this decrease is not observed in LiF, where the first moment of the F_3^+ centers band has a constant value within experimental sensitivity. As already discussed in Sec. II, the progressive shift of the PL peak position observed for ODC defects can be alternatively understood as a consequence of the dependence of the luminescence lifetime from the spectral position within the emission band. Hence, in Fig. 3(b) we report the values $\tau(E)$ of the PL lifetime as a function of the emission energy. The lifetimes were estimated for both PL activities by least-squares fitting data from time-resolved spectra [Fig. 1(a)] at different emission energies with an exponential function [$I(t)=I(0)e^{-t/\tau}$].²⁴ At this temperature (25 K), the decays are purely exponential for both activities.^{22,25} Figure 3(b) shows that the lifetime of Ge-ODC(II) centers in silica strongly varies within the emission band: τ goes from ~ 7.0 to ~ 10.7 ns. A similar behavior for Ge-ODC(II) was observed also under excitation by synchrotron radiation.²⁶ On the contrary, the lifetime of F_3^+ centers is almost constant in the observed range of emission energies. The above results were obtained exciting at the absorption peak for both PL activities. Although we performed the same measurements for different excitation energies within the absorption band, only a very weak dependence from this parameter was evidenced, consistent with previous results.²² Finally, to avoid any ambiguity on the interpretation of the present results due to potential coexistence of the overlapping PL activity of Si-ODC(II) in natural fused silica, we remark that results almost identical to those in Figs. 2 and 3 were obtained also on a sol-gel silica sample doped with 1000 ppm of Ge atoms, prepared as described in Ref. 21, where the intrinsic Si-ODC(II) optical activity is virtually absent.

V. DISCUSSION

The results in Fig. 3 qualitatively confirm the predictions of our theoretical analysis, i.e., that the dependence of the lifetime on the emission energy or, equivalently, the progressive redshift of the emission peak with time is a characteristic feature of luminescent defects embedded in a glassy matrix, as opposed to “crystalline” defects. We stress that the nonradiative decay channels are almost completely quenched for both PL signals at the temperature at which the experiments were performed (25 K).^{13,22} As a consequence, it is a very good approximation to consider the luminescence decay to be purely radiative. The main point of the following discussion is to fit all experimental data to our model and extract the values of the homogeneous and inhomogeneous widths of the PL emission bands and other interesting physical parameters.

For both investigated PL activities we have performed numerical integration of Eq. (9) to obtain a set of three theoretical curves which simultaneously fit: (i) the shape of the PL band at $t_D=0$, (ii) the time dependence of the first moment [calculated by using Eq. (10)], and (iii) the dependence of τ on emission energy.²⁷ To increase the reliability of the fit procedure, the half Stokes shift S was fixed at the value obtained experimentally by measuring the difference between the spectral positions of the absorption and emission peaks: $S=0.38$ eV and $S=0.24$ eV in silica and LiF, respectively. In this way, the fitting procedure was performed by varying only four free parameters, \widehat{E}_0 , σ_{in} , σ_{ho} , and γ . From the experimental point of view, the vibrational substructure of homogeneous luminescence bands cannot usually be resolved due to the bandwidth of the measuring system and to further broadening effects due for instance to the coupling with several low-energy modes. To take into account this effect, the homogeneous line shape, Eq. (8), was convoluted with a Gaussian distribution of a narrow half width $\hbar\omega_p$ before being inserted into Eq. (9).

The continuous lines in Figs. 2 and 3 represent the results of our fitting procedure. It is worth underlining the goodness of the fit, obtained using only four parameters, considering especially that data in Fig. 3 take into account simulta-

TABLE I. Upper section: Best-fitting parameters obtained by our theoretical model for the investigated PL activities. Lower section: Values of λ , σ_{tot} , $\hbar\omega_p$, H , and f as calculated from best-fitting parameters.

	\widehat{E}_0 (eV)	σ_{in} (meV)	σ_{ho} (meV)	S (eV)	γ ($10^6 \text{ eV}^{-3} \text{ s}^{-1}$)
I301	4.70 ± 0.05	177 ± 10	93 ± 12	0.38 ± 0.02	1.41 ± 0.09
LiF	2.50 ± 0.02	20 ± 10	109 ± 6	0.24 ± 0.02	10.0 ± 0.6
	λ (%)	σ_{tot} (meV)	$\hbar\omega_p$ (meV)	H	f
I301	78 ± 5	200 ± 10	23 ± 6	17 ± 5	0.073 ± 0.010
LiF	3 ± 2	111 ± 6	51 ± 7	5 ± 1	0.32 ± 0.04

neously all data acquired in a time-resolved PL measurement (typically ~ 600 spectral positions for each of the ~ 100 temporal acquisitions in Fig. 1). Table I summarizes the best parameters obtained via our fitting procedure for the two investigated PL activities. From the data in Table I, we can also calculate the Huang-Rhys factor $H=S^2/\sigma_{\text{ho}}^2$, the vibrational frequency $\hbar\omega_p=\sigma_{\text{ho}}/S$, the total half width (from $\sigma_{\text{tot}}^2=\sigma_{\text{in}}^2+\sigma_{\text{ho}}^2$),²⁸ and finally the parameter $\lambda=\sigma_{\text{in}}^2/\sigma_{\text{tot}}^2$, which estimates the degree of inhomogeneity. All these quantities are reported in Table I as well. As expected, λ is very small for the LiF defects in comparison with the amorphous ones: $\sim 3\%$ against $\sim 78\%$. These values correspond to σ_{in} being about 0.2 and 2 times of σ_{ho} in LiF and SiO₂, respectively. We note that the inhomogeneous broadening in the crystalline sample is not exactly zero; besides the approximations in our model, we note that a real crystal is always distorted by some dislocations, strains, or other imperfections distributed at random into the matrix. The obtained value of λ for Ge-ODC(II) shows that for a defect embedded in a glassy matrix, the inhomogeneous width can be prominent with respect to the homogeneous one. This conclusion may be at variance with previous suggestions that σ_{ho} and σ_{in} are typically comparable.¹⁴

In Fig. 2 we also show the discrete Poissonian homogeneous line shape of half width σ_{ho} and ZPL position \widehat{E}_0 , as obtained by our fit procedure for both investigated activities. As already pointed out, the crystalline PL band is completely described by the homogeneous shape,²⁹ whereas the silica PL band is not reproduced without taking into account inhomogeneous effects. It is also worth noting that the value $\hbar\omega_p=23 \pm 6$ meV obtained via our fitting procedure is very close to the value of 26 ± 2 meV found for the same defect by the analysis of the temperature dependence of the experimental absorption linewidth.³⁰ Moreover, $\hbar\omega_p$ is in good agreement with experimental and computational works on silica glasses which predict the presence of vibrational modes of low frequency.^{31,32} This agreement further confirms the correctness of the present value of σ_{ho} and consequently of our analysis.

To show the accuracy of our fitting procedure in determining λ , in Fig. 4 we compare the experimental lifetimes of Ge-ODC(II) in the I301 sample with the predictions of our model obtained for different λ values. The theoretical $\tau(E)$ curves are obtained by keeping σ_{tot} fixed at the value which best fits the overall experimental shape of the PL band. This

analysis clearly evidences a continuous transition from constant lifetimes for $\lambda=0$ (that is, a completely homogeneous PL band) to an inverse cubic dependence of τ from emission energy for $\lambda=1$ (that is, a completely inhomogeneous PL band), as anticipated in Sec. II. Finally, the oscillator strength f reported in Table I is calculated using³

$$f = \frac{2m_e}{3\hbar^2 e^2} \frac{1}{g_l} E_{\text{Abs}} |D|^2, \quad (12)$$

where m_e and e are, respectively, the mass and the charge of electron. We have substituted in Eq. (12) the value of $|D|^2$, calculated from the fitting parameter γ , and we have used for E_{Abs} the value \widehat{E}_0+S . In regard to the effective field correction, the term $\frac{1}{n} \left(\frac{E_{\text{eff}}}{E_{\text{ext}}}\right)^2$ calculated within the Onsager model^{1,3} turns out to be close to unity both in SiO₂ ($n \sim 1.5$) and in LiF ($n \sim 1.4$) in the investigated spectral range. The oscillator strength found here for Ge-ODC(II) in silica is consistent with the range of values reported in literature:¹⁴ 0.03–0.07. For F_3^+ centers in LiF, our result is close to 0.2 reported in Ref. 33.

The main assumption of our model that all amorphous effects can be completely accounted for by a simple Gaussian distribution of a single homogeneous parameter (i.e.,

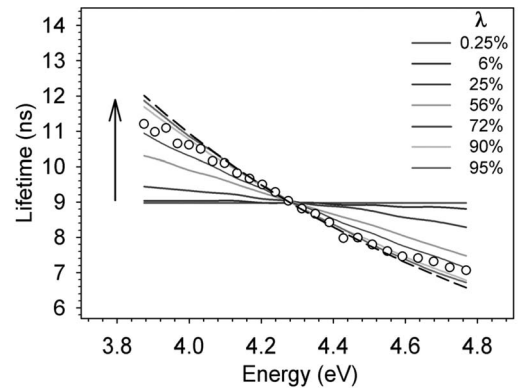


FIG. 4. Experimental decay lifetime at different emission energies for Ge-ODC(II) point defects (white circles); lifetime as predicted by our model for different values of the parameter λ (continuous lines). The dashed line represents the extreme case of $1/E^3$ dependence (see discussion). The arrow indicates the direction of increasing λ .

zero-phonon line) is strongly corroborated by the excellent agreement between theoretical curves and data. On the other side, a distribution of the emission peak E_0-S is strongly suggested *a priori* by the almost Einstein-type proportionality of $1/\tau$ on E^3 shown by experimental data in Fig. 4. Finally, it is important to note that in this scheme γ and thus $|D|^2$ are assumed as undistributed parameters. This means that the oscillator strength given by Eq. (12) can be distributed only as a consequence of the variations of E_{Abs} associated to different homogeneous absorption subbands.

VI. CONCLUSIONS

We have investigated the inhomogeneous properties of point defects in a glassy matrix via mapping by time-resolved PL the dependence of the radiative decay lifetime on emission energy. We propose a theoretical model, based on an extension of the standard theory of the optical properties of point defects, incorporating a statistical distribution of the zero-phonon line to account for the effects of the non-equivalent environments probed by each point defect in an amorphous matrix as opposed to a crystalline one. This model enlightens a direct connection between the dispersion of the radiative decay lifetime within a luminescence band as

a function of emission energy and the inhomogeneous properties of defects in a glassy environment. To confirm our prediction, we have experimentally studied the luminescence of oxygen deficient centers in silica and of aggregates of F centers in a crystalline sample of LiF. The model is able to fit all experimental data and to provide an estimate of the ratio $\lambda = \sigma_{\text{in}}^2 / \sigma_{\text{tot}}^2$ between the inhomogeneous and the total width, namely, $\sim 78\%$ for ODCs and $\sim 3\%$ for F_3^+ . Finally, our model allowed us to determine the homogeneous parameters of ODC and F_3^+ centers: homogeneous width, oscillator strength, Huang-Rhys factor, and the frequency of the vibrational local mode.

ACKNOWLEDGMENTS

We acknowledge financial support received from the project "P. O. R. Regione Sicilia-Misura 3.15-Sottoazione C." The authors would like to thank R. M. Montereali for having kindly provided the irradiated LiF sample. We also thank G. Lapis and G. Napoli for assistance in cryogenic work. Finally we are grateful to LAMP research group (<http://www.fisica.unipa.it/amorphous/>) for support and enlightening discussions.

*damico@fisica.unipa.it

¹A. M. Stoneham, *Theory of Defects in Solids* (Clarendon, Oxford, 1975), Vol. 1.

²*Silicon-based Materials and Devices*, edited by H. S. Nalwa (Academic, San Diego, CA, 2001).

³*Defects in SiO₂ and Related Dielectrics: Science and Technology*, edited by G. Pacchioni, L. Skuja, and D. L. Griscom (Kluwer, Dordrecht, 2000).

⁴*Persistent Spectral Hole-Burning: Science and Applications*, edited by W. E. Moerner (Springer-Verlag, New York, 1988).

⁵T. Itoh and M. Furumiya, *J. Lumin.* **48-49**, 704 (1991).

⁶U. Woggon, S. Gaponenko, W. Langbein, A. Uhrig, and C. Klingshirn, *Phys. Rev. B* **47**, 3684 (1993).

⁷D. M. Mittleman, R. W. Schoenlein, J. J. Shiang, V. L. Colvin, A. P. Alivisatos, and C. V. Shank, *Phys. Rev. B* **49**, 14435 (1994).

⁸L. Skuja, T. Suzuki, and K. Tanimura, *Phys. Rev. B* **52**, 15208 (1995).

⁹T. Kuroda, S. Matsushita, F. Minami, K. Inoue, and A. V. Baranov, *Phys. Rev. B* **55**, R16041 (1997).

¹⁰M. Leone, S. Agnello, R. Boscaino, M. Cannas, and F. M. Gelardi, in *Silicon-Based Materials and Devices*, edited by H. S. Nalwa (Academic, San Diego, 2001), Vol. 2, Chap. 1, p. 1.

¹¹Th. Förster, *Fluoreszenz Organischer Verbindungen* (Vandenhoeck und Ruprecht, Göttingen, 1951), p. 158.

¹²L. Vaccaro, M. Cannas, and R. Boscaino, *Solid State Commun.* **146**, 148 (2008).

¹³G. Baldacchini, E. De Nicola, R. M. Montereali, A. Scacco, and V. Kalinovic, *J. Phys. Chem. Solids* **61**, 21 (2000).

¹⁴L. Skuja, *J. Non-Cryst. Solids* **239**, 16 (1998).

¹⁵L. N. Skuja, A. N. Streletsky, and A. B. Pakovich, *Solid State*

Commun. **50**, 1069 (1984).

¹⁶A. Trukhin, B. Poumellec, and J. Garapon, *Radiat. Eff. Defects Solids* **149**, 89 (1999).

¹⁷M. Leone, S. Agnello, R. Boscaino, M. Cannas, and F. M. Gelardi, *Phys. Rev. B* **60**, 11475 (1999).

¹⁸A. Cannizzo, S. Agnello, R. Boscaino, M. Cannas, F. M. Gelardi, S. Grandi, and M. Leone, *J. Phys. Chem. Solids* **64**, 2437 (2003).

¹⁹A. Cannizzo and M. Leone, *Philos. Mag.* **84**, 1651 (2004).

²⁰Heraeus Quartzglas, Hanau, Germany, Catalog No. POL-0/102/E.

²¹S. Grandi, P. Mustarelli, S. Agnello, M. Cannas, and A. Cannizzo, *J. Sol-Gel Sci. Technol.* **26**, 915 (2003).

²²S. Agnello, R. Boscaino, M. Cannas, A. Cannizzo, F. M. Gelardi, S. Grandi, and M. Leone, *Phys. Rev. B* **68**, 165201 (2003).

²³E. Sonder and W. A. Sibley, in *Point Defects in Solids*, edited by J. H. Crawford and L. M. Slifkin (Plenum, New York, 1972), Vol. 1.

²⁴In regard to LiF, the fits were carried out in the range of $\sim 2.10-2.60$ eV so as to avoid the region of the F_3^+ emission band possibly affected by the overlap with the signal due to F_2^- .

²⁵G. Baldacchini, F. De Matteis, R. Francini, U. M. Grassano, F. Menchini, and R. M. Montereali, *J. Lumin.* **87-89**, 580 (2000).

²⁶S. Agnello, G. Buscarino, M. Cannas, F. Messina, S. Grandi, and A. Magistris, *Phys. Status Solidi C* **4**, 934 (2007).

²⁷The lifetimes predicted by the model were estimated by least-squares fitting the decay curves (not reported) predicted by Eq. (9) at different emission energies with a single exponential. It is worth noting that the simulated data (as real data) feature no appreciable nonexponential behavior in the time scale of experimental data, at least when the parameters of the model are close to the best-fit ones.

- ²⁸Alternatively, one can estimate σ_{tot} directly from experimental data, thus obtaining a consistent value.
- ²⁹As explained above, the homogeneous shape is obtained by a convolution of the discrete Poissonian with a narrow Gaussian curve of half width $\hbar\omega_p$ to take into account further homogeneous broadening effects and experimental bandwidth.
- ³⁰A. Cannizzo, S. Agnello, R. Boscaino, M. Cannas, F. M. Gelardi, S. Grandi, and M. Leone, *J. Phys. Chem. Solids* **64**, 2437 (2003).
- ³¹F. L. Galeener, A. J. Leadbetter, and M. W. Stringfellow, *Phys. Rev. B* **27**, 1052 (1983).
- ³²P. Umari, X. Gonze, and A. Pasquarello, *Phys. Rev. Lett.* **90**, 027401 (2003).
- ³³T. Kurobori, T. Kanasaki, Y. Imai, and N. Takeuchi, *J. Phys. C* **21**, L397 (1988).